Estimating Radar Detection Coverage Probability of Targets in a Cluttered Environment Using Stochastic Geometry

by

Gaurav Singh

A thesis submitted in partial fulfillment for the
degree of Master of Technology

under supervision of
Dr. Shobha Sundar Ram
Department of Electronics and Communication Engineering
Indraprastha Institute of Information Technology, Delhi

July 2020

Estimating Radar Detection Coverage Probability of Targets in a Cluttered Environment Using Stochastic Geometry

by

Gaurav Singh

A thesis submitted in partial fulfillment for the
degree of Master of Technology

to

Indraprastha Institute of Information Technology, Delhi

July 2020

Certificate

This is to certify that the thesis titled "Estimating Radar Detection Coverage Probability of Targets in a Cluttered Environment Using Stochastic Geometry" being submitted by Gaurav Singh (Roll No.- MT18160) to the Indraprastha Institute of Information Technology Delhi, for the award of the Master of Technology, is an original work carried out by him under my supervision. In my opinion, thesis has reached the standards fulfilling the requirements of the regulations relating to the degree. The results contained in the thesis have not been submitted in part or full to any other university or institute for the award of any degree/diploma.

Date: _____

Dr. Shobha Sundar Ram
Head & Associate Professor
Department of Electronics and Communication Engineering
Indraprastha Institute of Information Technology, Delhi
New Delhi 110020

Abstract

We analyze the performance of a radar in an environment where clutter is constituted by discrete scatterers whose radar cross-sections are comparable to that of the target. An indoor radar deployment to detect humans in the presence of furniture is an example of such a scenario. We propose a figure of merit called the radar detection coverage probability (P_{DC}) to indicate the likelihood of the signal to clutter and noise ratio at the radar being above a predefined threshold under diverse radar, target and clutter conditions. We provide analytical expressions derived from stochastic geometry formulations to derive the P_{DC}. Based on our analyses, we find useful insights regarding the optimal choice of the transmitted power and radar bandwidth. We also study the sensitivity of the performance of the radar to clutter density, clutter cross-section and path loss under both line-of-sight and non-line-of-sight conditions. Our results are verified through Monte Carlo simulations and Finite Difference Time Domain (FDTD) solver.

Acknowledgements

I would like to express my sincere gratitude to Dr. Shobha Sundar Ram for giving me the opportunity to work on my thesis under her guidance. Her advice, expertise and experience have been invaluable for my entire research work as well as my career.

I would also like to thank Dr. Gourab Ghatak for his assistance and expertise on the subject which he offered during this work.

I am grateful to my parents for supporting me with love and guidance for my career.

Contents

List of Figures

List of Tables

List of Symbols

Symbol	Description
λ	Wavelength of radar
P_{tx}	Transmitted power
$G(\theta)$	Antenna gain at an angle θ
σ_c	Clutter radar cross section
σ_0	Mean physical size of clutter
σ_t	Target radar cross section
N	Receiver noise
BW	Radar Bandwidth
P_{DC}	Radar detection coverage probability
γ	Threshold of detection
q	Path loss coefficient
ΔR	Radar range resolution
R_f	Far field distance of radar
R_t	Distance of target from radar
r_c	Distance of clutter from radar

Chapter 1

Introduction

The performance of a radar can significantly deteriorate in the presence of elements, or clutter, that occupy the same range resolution cell as that of the target, resulting in unwanted backscattered signals [1]. Depending on the application, different types of clutter may be encountered, such as surface clutter due to reflections from the ground, or sea and volumetric clutter from rain. In this work, we consider a specific type of clutter that arises from a collection of discrete scatterers whose physical sizes are comparable to the size of the targets. For example, trees, animals, birds and insects in ground-based outdoor surveillance radars, environmental features such as buildings and road signs for automotive radars, or furniture and walls in the case of indoor radars. Traditionally, where the objective is to track moving targets, static clutter is eliminated through high pass filtering of the time-domain data. Further, returns from discrete clutter scatterers are mitigated directly in the radar signatures using techniques such as CLEAN [2] and RELAX [3]. More recently, clutter arising from multipath signals from discrete scatterers have been exploited for imaging the target in non-line-of-sight scenarios [4]. In our work, we specifically focus on the detection performance of the radar in the presence of clutter before any type of post processing of radar data, is carried out.

In the radar scenarios consisting of discrete scatterers, there can be considerable diversity in the position and distribution of the scatterers, in the radar cross-section of the scatterers, and in the propagation physics between the radar and target. In case the cost and effort of radar data collection are not prohibitive, useful insights regarding the performance of the radar can be gathered from empirical studies, which are based on actual radar deployments. Radar models of clutter phenomenology present a cost effective alternative for studying the detection performance and for establishing thresholds for constant false alarm radars. Modeling of radar phenomenology using full

wave electromagnetic solvers such as finite difference time domain techniques, finite element methods or even less accurate techniques based on ray tracing are computationally very expensive, especially for spatially large regions. Additionally, these electromagnetic solvers do not inherently capture the stochastic nature of the channel, radar and target conditions. Statistical models such as Rayleigh, log-normal, Weibull and k-distribution have been extensively explored in radar literature to describe different types of clutter from sea, ground, trees and rain for different operating frequencies and polarization [5]. For a given range resolution cell of the radar, if the target and the clutter backscatter are respectively S and C and the noise power is N, then the signal to clutter and noise ratio (SCNR) is $S/(C+N)$. In this work, we present an analytical framework based on stochastic geometry to study the detection performance of the radar limited by SCNR due to backscatter signals from discrete scatterers in the environment of the target.

Stochastic geometry [6] has been extensively applied in wireless networks to characterize performance metrics such as coverage probability and connectivity of cellular networks [7], millimeter wave networks [8], multi-radio access technique networks [9] and vehicular communications systems [10]. In these works, the system parameters were determined as a function of the signal to interference and noise ratio (SINR) where the interference may arise from neighbouring base stations (in the case of cellular networks) or other wireless transmitters (in ad hoc networks). More recently, stochastic geometry tools were used to obtain close form expressions for the detection performance of radar in the presence of interference from neighbouring radars. The study was performed in the context of automotive radars in [11] and for a network of short range low cost radars in [12].

In noise-limited radar scenarios, the signal to noise ratio is the key figure of merit. On the other hand, in clutter limited scenarios, SCNR will determine the performance of the radar. In this work, we propose a figure of metric called the radar detection coverage probability ($P_{DC}(r)$) as the probability that the mean SCNR is above a specified threshold (γ). The metric is analogous to coverage probability in wireless communication networks which is the probability that a typical mobile user is able to achieve an SINR that is above a specified threshold [6].

In the radar scenarios where there are numerous discrete scatterers that constitute the clutter, the clutter backscatter is governed by a number of stochastic processes including the random spatial distribution of the scatterers, the radar cross-section of each of the scatterers, absorption, shadowing and fading. Consequently, in this work, we model the positions of the scatterers as a two-dimensional Poisson point process (PPP) [13]. This implies that the number of scatterers in a closed subset of the two-dimensional space follows a Poisson distribution across multiple trials. Furthermore, conditioned on the

number of scatterers, the position of these scatterers follow a uniform distribution inside that subset. Previous works have similarly modeled discrete clutter as a PPP for multi-target tracking [14]. The radar cross-section of these scatterers are assumed to follow a standard Swerling cross-section model [15]. Then, using tools from stochastic geometry, we estimate the SCNR for a target at a distance r from a monostatic impulse radar based on the transmitted power, gains of the radar antennas, radar range resolution and the radar receiver noise. The analytical formulations present significant reduction in the computational complexity especially in comparison to the alternative of running multiple deterministic models based on full wave electromagnetic solvers. All the results are verified with Monte Carlo simulations. Finally, our results show that the metric presents useful insights on tuning important radar parameters such as the transmitted power, the bandwidth and the gain of the radar antennas. For example, our results show that the P_{DC} asymptotically converges to a maximum with increase in the transmitted power and further increase in power does not improve the detection performance of the radar. We also show the optimum bandwidth for realizing peak SCNR.

1.0.1 Structure of the Work

This thesis is divided in 5 chapters.

- **Chapter 2: Theory**
  This chapter covers all the formulations and theorems worked out. Analysis of Radar equations is done with Stochastic Geometry manipulations.
- **Chapter 3: Experimental Set Up**
  This chapter specifies the Radar parameters, the target and clutter specifications. Values taken for the experiment are defined.
- **Chapter 4: Experimental Results**
  In this chapter results and analysis is done on the various outcomes. Changes in the introduced metric is studied by varying different parameters and conclusions are drawn.
- **Chapter 5: Validation of Stochastic Geometry results**
  The validation of the results and the algorithms are discussed in this chapter. There are two sections that discuss Monte Carlo and FDTD methods respectively.

Chapter 2

Theory

We consider two scenarios. In the first scenario, the target is in the line of sight of the radar at a range R_t while the discrete clutter scatterers fall outside of the radius R_t as shown in Fig. 2.1a. In the second scenario, we assume that the target is not within the LOS of the radar as shown in Fig. 2.1b.

2.0.1 Target in Line of Sight

Consider a monostatic impulse radar of wavelength λ_c located at the origin of a two dimensional circular space.

The transmitted power from the radar is P_{tx}. We assume that the radar consists of directional transmitting and receiving antennas of gain $G_{tx}(\theta)$ and $G_{rx}(\theta)$ respectively where θ is the direction-of-arrival of a direct path signal from a point scatterer. We consider that the clutter consists of a collection of discrete scatterers distributed randomly in the two-dimensional space. For example, the trees in a forest in the case of a foliage

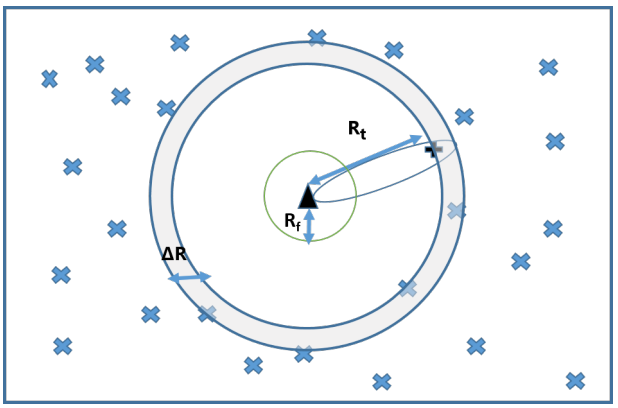

a. Target is in LOS with respect to radar

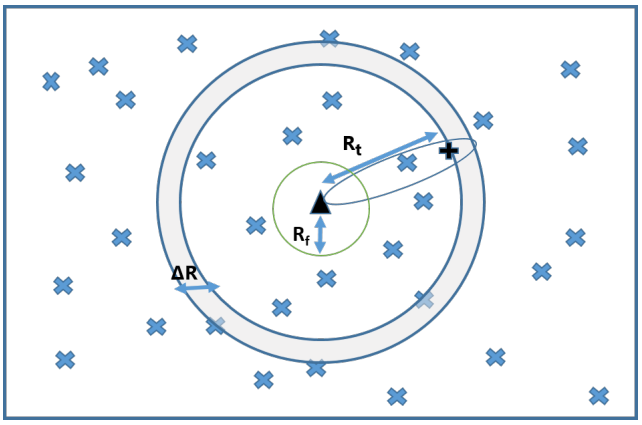

b. Target is in NLOS with respect to radar

FIGURE 2.1: Monostatic radar of transmitting power P_{tx}, gain $(G(\theta))$, range resolution (ΔR), system noise temperature (T_S), at center with target of average cross-section (σ_t) at (R, θ_t) of such that $G(\theta_t) = 1$. Clutter constituted by discrete scatterers of average cross-section (σ_c) modeled as homogeneous PPP.

penetration radar or the furniture in a room for an indoor radar. We have indicated the clutter as crosses in the figure. The nearest distance between the scatterers constituting the clutter and the radar is assumed to be R which we assume is below the maximum unambiguous range of the radar determined by the pulse repetition frequency. In order to evaluate the performance of the radar while accounting for the diversity in the clutter conditions, we model the positions of the scatterers as a PPP Φ' defined on the domain $\mathbb{R}^2 \backslash \mathcal{B}(0, R)$, where $\mathcal{B}(0, r)$ represents a circle of radius R centered around the origin. The position of each scatterer c is denoted in polar coordinates as $\vec{\mathbf{r}}_c = (\mathbf{r_c}, \theta_\mathbf{c})$. These scatterers are assumed to be uniformly distributed in azimuth $\theta_\mathbf{c} \in [0, 2\pi)$ and range $\mathbf{r_c} \in (R, \infty]$. The expectation of the number of scatterers of the point process is the intensity measure $\mathcal{P}(d\vec{r}_c)$ which is finite. In our work, we assume a homogeneous PPP, where $\mathcal{P}(d\vec{r}_c) = \rho d\vec{r}_c$ where $d\vec{r}_c$ is the unit two-dimensional space and ρ is the clutter density[1]. We assume an exponential distribution for the radar cross-section of each discrete scatterer $(\sigma_\mathbf{c})$ contributing to clutter given by

$$P(\sigma_\mathbf{c}) = \frac{1}{\sigma_{\mathbf{c}_{\text{avg}}}} exp\left(\frac{-\sigma_\mathbf{c}}{\sigma_{\mathbf{c}_{\text{avg}}}}\right), \tag{2.1}$$

where $\sigma_{c_{avg}}$ is the average clutter cross-section. Based on the radar range equation, the total clutter power received at the radar for each realization of the PPP is

$$\mathbf{C} = \sum_{c \in \Phi'} \frac{KG(\theta_\mathbf{c})\sigma_\mathbf{c} g_c}{{\mathbf{r_c}}^{2q}} \tag{2.2}$$

[1]Naturally, $\mathcal{P}(d\vec{r}_c) = 0$ for $0 \leq \mathbf{r_c} \leq R$.

where K is a constant and is equal to $\frac{P_{tx}\lambda^2}{(4\pi)^3}$, $G(\theta_{\mathbf{c}}) = G_{tx}(\theta_{\mathbf{c}})G_{rx}(\theta_{\mathbf{c}})$, $\mathbf{g_c}$ is a random variable that models the fading / interference between the different clutter returns and q is the path loss exponent.

The target, indicated as a plus in the figure, is within the line-of-sight of the radar. Hence, the target position $(\mathbf{r_t}, \theta_\mathbf{t})$ can range from $\mathbf{r_t} \in (R_f, R]$ where R_f is the far-field Fraunhofer radius of the radar antennas. The target azimuth, $\theta_\mathbf{t}$, is assumed to lie within the main lobe of the radar which can lie anywhere from $[0, 2\pi)$. For a target cross-section of $\sigma_\mathbf{t}$, the received signal at the radar for a single pulse is

$$\mathbf{S} = \frac{KG(\theta_\mathbf{t})\sigma_\mathbf{t}}{{\mathbf{r_t}}^{2q}}, \tag{2.3}$$

where $G(\theta_\mathbf{t}) = G_{tx}(\theta_\mathbf{t})G_{rx}(\theta_\mathbf{t})$. We assume a Swerling-1 RCS fluctuation for the target given by

$$P(\sigma_\mathbf{t}) = \frac{1}{\sigma_{\mathbf{t}_{\text{avg}}}} exp\left(\frac{-\sigma_\mathbf{t}}{\sigma_{\mathbf{t}_{\text{avg}}}}\right), \tag{2.4}$$

where $\sigma_{\mathbf{t}_{\text{avg}}}$ is the average target cross-section.

Under line-of-sight conditions, the minimum SCNR is obtained when $\mathbf{r_t} = R$. If we assume that the radar tracks the target such that the latter always falls within its main beam, then $G(\theta_t) = 1$. Therefore, the average SCNR for a given R is

$$\mathbb{E}\left[\mathbf{SCNR}(R)\right] = \mathbb{E}_{\sigma_t,\sigma_c,g_c,\Phi'}\left[\frac{\frac{K\sigma_\mathbf{t}}{R^{2q}}}{N + \sum_{\mathbf{c}\in\Phi}\frac{KG(\theta_\mathbf{c})\sigma_\mathbf{c}\mathbf{g_c}}{{\mathbf{r_c}}^{2q}}}\right]. \tag{2.5}$$

The resulting SCNR presented above is a stochastic function that is determined by multiple random variables. In order to study the detection performance of the radar, we define a metric as follows:

Definition 2.1. The radar detection coverage probability, $P_{DC}(r)$, of a target for a distance r is defined as the probability that the average SCNR at r is greater than or equal to a predefined threshold (γ).

$$P_{DC}(r) \triangleq \mathbb{P}\left(\mathbf{SCNR}(r) \geq \gamma\right). \tag{2.6}$$

In the following theorem, we mathematically characterize $P_{DC}(r)$.

Theorem 2.2. *The radar detection coverage probability for a target located at LOS distance R from the radar within the field of view of the radar such that $G(\theta_t) = 1$ is*

given by:

$$P_{DC}(R) = I(R) exp\left(\frac{-\gamma N R^{2q}}{K\,\sigma_{\mathrm{t_{avg}}}}\right), \tag{2.7}$$

where,

$$I(R) = exp\left(-\rho \int_0^{2\pi} \int_R^{R+\Delta R} \frac{\nu(R) G(\theta_c) r_c}{\nu(R) G(\theta_c) + r_c^{2q}} dr_c d\theta_c\right), \tag{2.8}$$

and $\nu(R) = \frac{\gamma R^{2q}\,\sigma_{\mathrm{c_{avg}}}}{\sigma_{\mathrm{t_{avg}}}}$.

Proof. From the definition of $P_{DC}(R)$, we have:

$$\begin{aligned} P_{DC}(R) &= \mathbb{P}\left[\sigma_t > \frac{\gamma N R^{2q}}{K} + \gamma R^{2q} \sum_{\mathbf{c}\in\Phi} \frac{G(\theta_{\mathbf{c}})\sigma_{\mathbf{c}}\mathbf{g_c}}{{\mathbf{r_c}}^{2q}}\right] \\ &\overset{(a)}{=} \mathbb{E}_{\sigma_c, g_c, \Phi'}\left[exp\left(\frac{-\gamma N R^{2q}}{K\,\sigma_{\mathrm{t_{avg}}}} - \frac{\gamma R^{2q}}{\sigma_{\mathrm{t_{avg}}}} \sum_{\mathbf{c}\in\Phi} \frac{G(\theta_{\mathbf{c}})\sigma_{\mathbf{c}}\mathbf{g_c}}{{\mathbf{r_c}}^{2q}}\right)\right] \\ &\overset{(b)}{=} exp\left(\frac{-\gamma N R^{2q}}{K\sigma_{t_{avg}}}\right) \mathbb{E}_{\sigma_c, g_c, \Phi'}\left[\prod_{\mathbf{c}\in\Phi} exp\left(\frac{-\gamma R^{2q} G(\theta_{\mathbf{c}})\sigma_{\mathbf{c}}\mathbf{g_c}}{\sigma_{\mathrm{t_{avg}}}\,{\mathbf{r_c}}^{2q}}\right)\right]. \end{aligned} \tag{2.9}$$

The step (a) follows from the fact that the target cross-section is based on a Swerling-1 model, as shown in (2.4). The expectation is with respect to the scatterers constituting the clutter, their spatial distribution, their cross-section, and their mutual interference. The step (b) is from the fact that the exponential of sums equals the product of exponential functions. Now the expectation in (b) is evaluated using the probability generating functional of Φ [13], as follows:

$$\begin{aligned} &\mathbb{E}_{\sigma_c, g_c, \Phi'}\left[\prod_{c\in\Phi'} exp\left(\frac{-\gamma R^{2q} G(\theta_{\mathbf{c}})\sigma_{\mathbf{c}}\mathbf{g_c}}{\sigma_{\mathrm{t_{avg}}}\,{\mathbf{r_c}}^{2q}}\right)\right] = \\ &exp\left(-\rho \int_{\mathbb{R}^2} \left(1 - \mathop{\mathbb{E}}_{\sigma_{\mathbf{c}}, \mathbf{g_c}}\left[exp\left(-\frac{\gamma R^{2q} G(\theta_c)\sigma_{\mathbf{c}}\mathbf{g_c}}{\sigma_{\mathrm{t_{avg}}}\, r_c^{2q}}\right)\right] d(\vec{r}_c)\right)\right). \end{aligned} \tag{2.10}$$

The expectation inside the integral is with respect to the interference term ($\mathbf{g_c}$) and the scatterer cross-section (σ_c). Under worst case scenarios, i.e., when $\mathbf{g_c} = 1$, the signals from all the scatterers add constructively to give rise to the highest clutter returns. If we assume an exponential distribution of the scatterer cross-section as given in (2.1),

then

$$\begin{aligned}\mathop{\mathbb{E}}_{\sigma_{\mathbf{c}},\mathbf{g_c}}\left[exp\left(-\frac{\gamma R^{2q} G(\theta_c)\sigma_{\mathbf{c}}\mathbf{g_c}}{\sigma_{\mathrm{t_{avg}}}\, r_c^{2q}}\right)\right] &= \frac{1}{1+\frac{\gamma R^{2q} G(\theta_c)\,\sigma_{\mathrm{c_{avg}}}}{\sigma_{\mathrm{t_{avg}}}\, r_c^{2q}}} \\ &= \frac{1}{1+\frac{\nu(R) G(\theta_c)}{r_c^{2q}}},\end{aligned} \tag{2.11}$$

where $\nu(R) = \frac{\gamma R^{2q}\,\sigma_{\mathrm{c_{avg}}}}{\sigma_{\mathrm{t_{avg}}}}$. The result in (2.7) follows from substituting (2.11) in (2.10). Note that we have only considered the clutter from scatterers that lie within the same range resolution cell as the target between R and $R + \Delta R$ where $\Delta R = \frac{c}{2BW}$, the range resolution is estimated from the bandwidth (BW) of the radar. If multipath components from scatterers arising from other range cells must be considered, then the clutter equation in (2.2) can be modified for a higher order q (path loss coefficient) and the integral limits for r_c in (2.8) can be extended from R to ∞. □

2.0.2 Target in Non-Line-of-Sight Conditions

We consider a second scenario shown in Fig. 2.1b. In NLOS conditions, the radar signal to the target may be exponentially decayed due to propagation through the material of the clutter scatterers. This decay function must be incorporated in the propagation loss function. The target can be detected when the signal to clutter and noise ratio at the range cell occupied by the target is greater than or equal to a threshold. In the recent developments in urban radars and around-the-corner radars [16], targets are being detected based on their multipath scattered signals reflected off the surface of the scatterers at *other* range cells not occupied by the target. In our current discussion, we do not consider those cases. We consider a two-dimensional space with the radar at the origin. The clutter consists of a set of discrete scatterers, indicated as crosses in the figure, whose positions ($\vec{r_c} = \mathbf{r_c}, \theta_\mathbf{c}$) follow a PPP Φ defined in $\mathbb{R}^2$. We assume that the target, indicated as a plus in the figure, is located at $\vec{r_t} = (r_t, \theta_t)$. The region between the radar and the target may consist of multiple scatterers which attenuate the propagating signal. The attenuation factor due to the material properties of the scatterer is assumed to be $\alpha(\lambda_c)$ which is a function of the carrier frequency or wavelength of the radar. Since the region between the radar and the target is partially covered with clutter, the attenuation α is factored with $\rho\sigma_0$ where ρ is the intensity measure of the PPP while σ_0 is the average (two-dimensional) physical area occupied by the scatterers. In other words, the average attenuation of the propagating signal, $\alpha' = \alpha\rho\sigma_0$, is determined by the material properties of the medium, the number of scatterers (governed by ρ) and the size of the scatterers (governed by σ_0). The received signal from the target is therefore

given by

$$\mathbf{S} = \frac{KG(\theta_t)\sigma_{\mathbf{t}}e^{-2\alpha' r_t}}{r_t^{2q}} \tag{2.12}$$

Similarly the clutter returns are

$$\mathbf{C} = \sum_{\mathbf{c}\in\Phi} \frac{KG(\theta_{\mathbf{c}})e^{-2\alpha'\mathbf{r_c}}\sigma_{\mathbf{c}}g_c}{{\mathbf{r_c}}^{2q}}. \tag{2.13}$$

Theorem 2.3. *The radar detection coverage probability of a target at any NLOS distance r_t from the radar within the field of view of the radar such that $G(\theta_t) = 1$ is given by*

$$P_{DC}(r_t) = J(r_t)exp\left(\frac{-\gamma N r_t^{2q} e^{2\alpha' r_t}}{K\,\sigma_{\mathrm{t_{avg}}}}\right) \tag{2.14}$$

where

$$\begin{aligned} &J(r_t) = \\ &exp\left(-\rho\int_0^{2\pi}\int_{r_t}^{r_t+\Delta R}\frac{\nu'(r)G(\theta_c)r_c}{\nu'(r)G(\theta_c)+r_c^{2q}e^{2\alpha' r_c}}dr_c d\theta_c\right) \end{aligned} \tag{2.15}$$

and

$$\nu'(r_t) = \frac{\gamma r_t^{2q} e^{2\alpha' r_t}\,\sigma_{\mathrm{c_{avg}}}}{\sigma_{\mathrm{t_{avg}}}}. \tag{2.16}$$

Proof. From the definition of the radar detection coverage probability, we have

$$\begin{aligned} &P_{DC}(r_t) = \mathbb{P}\left[\mathbf{SCNR}(r_t) > \gamma\right] = \\ &\mathbb{P}\left[\frac{\frac{K\sigma_{\mathbf{t}}}{r_t^{2q}}e^{-2\alpha' r_t}}{N+\sum_{\mathbf{c}\in\Phi}\frac{KG(\theta_{\mathbf{c}})\sigma_{\mathbf{c}}\mathbf{g_c}}{{\mathbf{r_c}}^{2q}}e^{-2\alpha'\mathbf{r_c}}} > \gamma\right]. \end{aligned} \tag{2.17}$$

We repeat the steps of stochastic geometry in an identical manner to what were presented in equations (2.9) to (2.11), in order to obtain the result. The detection probability can be estimated through numerical integration of (2.15). □

Chapter 3

Experimental Set Up

We consider an indoor radar scenario where the radar operates at 5GHz. We assume that the transmitted power, the radar bandwidth and the gain of the antennas can be varied. We assume that the radar consists of a uniform linear array of N_a elements that are spaced half wavelength apart. Therefore, the gain of the antenna is given by

$$G(\theta) = G_{rx}(\theta)G_{tx}(\theta) = \left[\frac{\sin\left(\frac{N_a\pi}{2}\cos\theta\right)}{\sin\left(\frac{\pi}{2}\cos\theta\right)}\right]^2. \tag{3.1}$$

The Fraunhofer far-field radius of this antenna can be estimated from the dimensions of the antenna and the radar wavelength $\left(R_f = \frac{2(N_a-1)^2}{\lambda_c}\right)$. The mean noise power (N) is computed from the product of the Boltzmann constant, the system noise temperature (T_s) and radar bandwidth (BW). We assume a system noise temperature of $76K$. The indoor furniture which constitute the clutter scatterers are assumed to be mostly made of wood with a mean radar cross-section of $0.1m^2$. The mean physical area of the clutter scatterers is also assumed to be $\sigma_0 = 0.1m^2$. The density of the clutter ρ which shows the mean number of furniture pieces in a square meter of the indoor area is assumed to vary from 0.01 to 1 per square meter. The attenuation of the carrier signal through the material of the scatterer is assumed to be approximately $\alpha = 20Np/m$. Therefore, the mean attenuation through the clutter to a target under NLOS conditions is $\alpha' = \alpha\rho\sigma_0$ where $\rho\sigma_0$ show the fraction of occupancy of a unit area by clutter scatterers. The radar and channel parameters are summarized in Table. 3.1.

TABLE 3.1: Radar Parameters

Parameters	Values
Radar wavelength (λ)	6cm
Radar Bandwidth (BW)	10 MHz to 2GHz
Transmitted power (P_{tx})	-20 to 50 dBm
Receiver noise power (N)	-120 to -90 dBm
Gain (dBi)	0 to 20dBi
Mean physical size of clutter scatterer (σ_0)	$0.1m^2$
Clutter Density (ρ)	$\frac{0.01}{m^2}$ to $\frac{0.1}{m^2}$
Average clutter cross-section ($\sigma_{c_{avg}}$)	0.01 to $1m^2$
Average target cross-section ($\sigma_{t_{avg}}$)	$0.1m^2$
Path loss coefficient (q)	2 to 3
Threshold (γ)	1

Chapter 4

Experimental Results

In the following section, we discuss the experimental results obtained from the stochastic geometry analysis presented in the previous sections. The performance of the radar is governed by the radar parameters such as transmitted power, receiver bandwidth, the gain of the antennas and the noise temperature of the receiver as well as clutter parameters such as clutter density and mean clutter cross-section. We study the effect of the two sets of the parameters below.

4.0.1 Effect of clutter parameters

First, we consider the effect of the clutter density on the performance of the radar. In our study ρ is the intensity measure of the scatterers in the two-dimensional space. We study the performance in both LOS and NLOS scenarios and present the results in Fig.4.1.

In this analysis, P_{tx}, the noise figure ($[F]$), the gains of the antennas and the bandwidth are assumed to be $+30dBm$, $1dB$, $0dBi$ and 150MHz respectively. We vary the ρ from 0 to 0.1 and display the P_{DC} for different target distances in the far field ($R > R_f$). When ρ is zero, then the SCNR reduces to SNR due to absence of clutter backscatter. Since there are no clutter scatterers blocking the target from the radar, the NLOS scenario is identical to the LOS scenario as $\alpha' = 0$. The figure shows that in the absence of clutter backscatter, the P_{DC} remains high for very large distances (up to 30m). However, the introduction of clutter quickly deteriorates the performance of the radar. Higher the value of clutter, the poorer the performance of the radar. The performance in NLOS scenario is comparable to the LOS scenario. This is an unexpected outcome and it follows from the fact that in NLOS scenarios, the path loss to the target and the clutter,

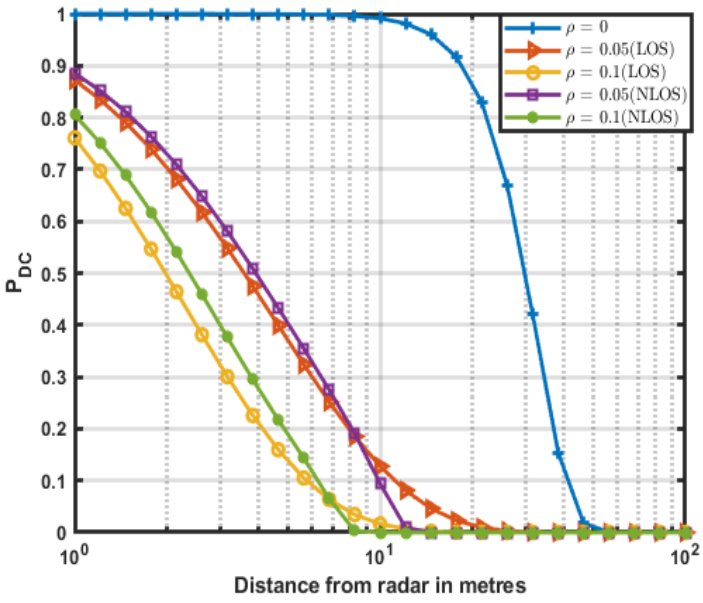

FIGURE 4.1: Variation of P_{DC} with target distance (R) for different clutter densities. Mean clutter cross-section and radar parameters are kept fixed.

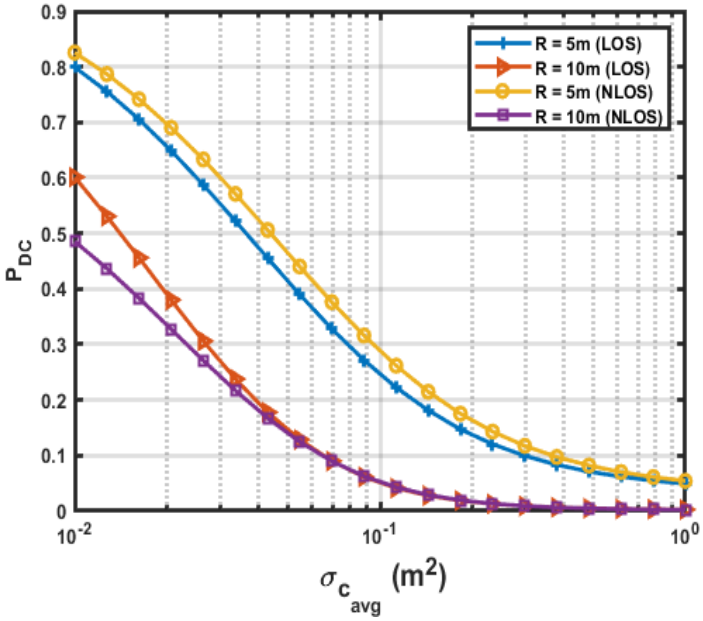

FIGURE 4.2: Variation of P_{DC} with target distance (R) for different mean clutter cross-sections. Clutter density and radar parameters are kept fixed.

both, experience attenuation. Hence, the SCNR in some NLOS situations may be higher than that of the LOS situations.

Next, we consider the effect of the mean clutter cross-section on the performance of the radar in Fig.4.2. All the radar parameters are left unchanged. We fix ρ to be $0.1/m^2$ and plot P_{DC} for difference values of $\sigma_{c_{avg}}$ from $0.001m^2$ to $1m^2$. The mean physical size of

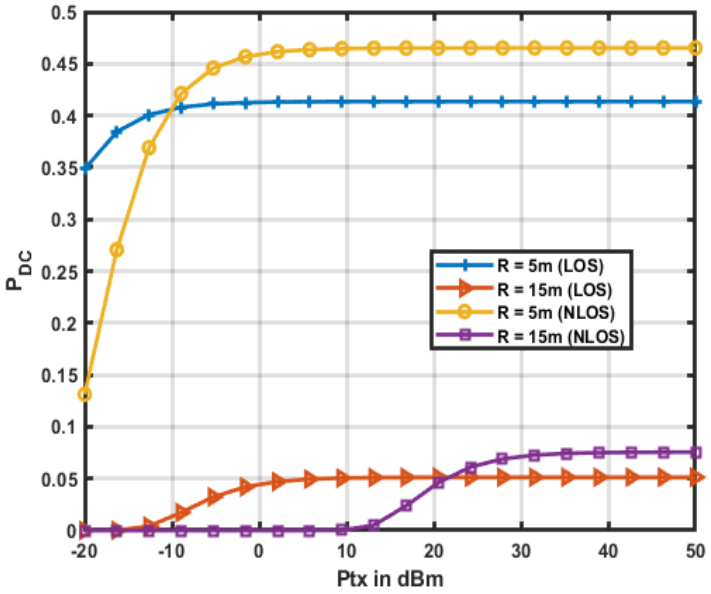

FIGURE 4.3: Variation of P_{DC} with transmitted power P_{tx} for different target distances. Remaining radar parameters and clutter parameters are kept fixed.

the clutter is kept constant. This means that the reflectivity of the clutter scatterers are changed. We observe that for both LOS and NLOS, P_{DC} reduces for increase in $\sigma_{c_{avg}}$. The performance at farther distance $R = 10m$ is poorer than the performance at near distance $R = 5m$. Interestingly, the NLOS performs slightly better than the LOS at the near distance but is slightly worse than LOS at the farther distance. Again, this is because both target and clutter backscatter are affected by the exponential decay in the path loss due to the presence of clutter scatterers. In other words, some clutter scatterers may partially block the other scatterers. However, note that in real world conditions NLOS scenarios may have a greater path loss coefficient q than LOS scenarios due to fading as well as affected by the clutter density. The appropriate q for a specific clutter density is usually determined through emperical studies. In our study, we have assumed that q is same for both and is independent of ρ.

4.0.2 Effect of Radar Parameters

In this section, we keep the clutter parameters fixed ($\rho = 0.1/m^2, \sigma_{c_{avg}} = 0.2m^2$) in the analysis and study the effect of radar parameters on the performance. First, we consider the effect of the transmitted power which is varied from $-20dBm$ to $+50dBm$ in Fig.4.3. We observe that P_{DC} improves with increase in P_{tx} only up to a point. When radar returns are clutter limited, then there is no further improvement with higher P_{tx}. Again, for the same P_{tx}, the performance at farther distance ($R = 15m$) is poorer than the performance at near distance ($R = 5m$). We also observe, that NLOS

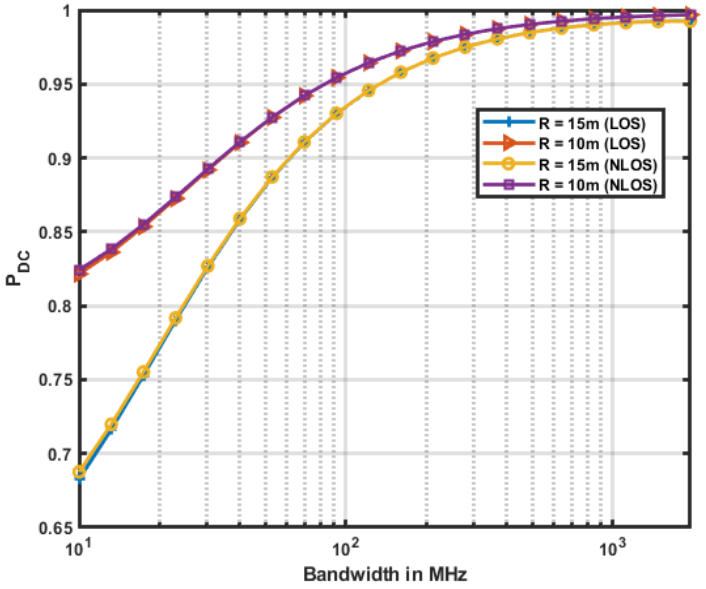

FIGURE 4.4: Variation of P_{DC} with receiver noise bandwidth (BW) for fixed noise figure. Remaining radar parameters and clutter parameters are kept fixed. Results shown for stochastic geometry (SG) formulations and Monte Carlo(MC) simulations.

scenario results in poorer performance than LOS at low P_{tx} when the performance is noise limited. However, at higher P_{tx} when the performance is clutter limited, the NLOS performance is slightly better than the LOS scenario.

The effect of bandwidth on the radar performance is observed in Fig.4.4. Here, $P_{tx} = 0dBm$ and the noise figure at $[F] = 0.01dB$. We vary the bandwidth from 10MHz to 2GHz. As the bandwidth increases, the receiver noise increases. However, the radar range resolution window is inversely proportionate to the bandwidth. For greater bandwidths, the lower range resolution (ΔR) results in lesser occupancy of clutter scatterers within the range window of the target. As a result, we observe that for every R, there is a peak performance for a specific bandwidth. At lower bandwidths, the clutter backscatter is high and at higher bandwidths, the noise becomes high. We have verified the results in the later section using Monte Carlo simulations.

In all of the results presented so far, the antennas have been assumed to be omnidirectional with $0dBi$ gain. Now, we study the effect of gain on the performance of the radar in Fig.4.5.

Here, P_{tx} is fixed at $30dBm$, $[F] = 0.01dB$, BW is 150MHz, $\rho = 0.01/m^2$ and $\sigma_{c_{avg}} = 0.1m^2$. The target is assumed to be in the mainlobe while the clutter scatterers may fall within the mainlobes as well as some of the sidelobes. The result show that the performance of the system improves with increase in gain. Since, the target is always assumed to be at the peak antenna gain, the target backscatter increases with gain.

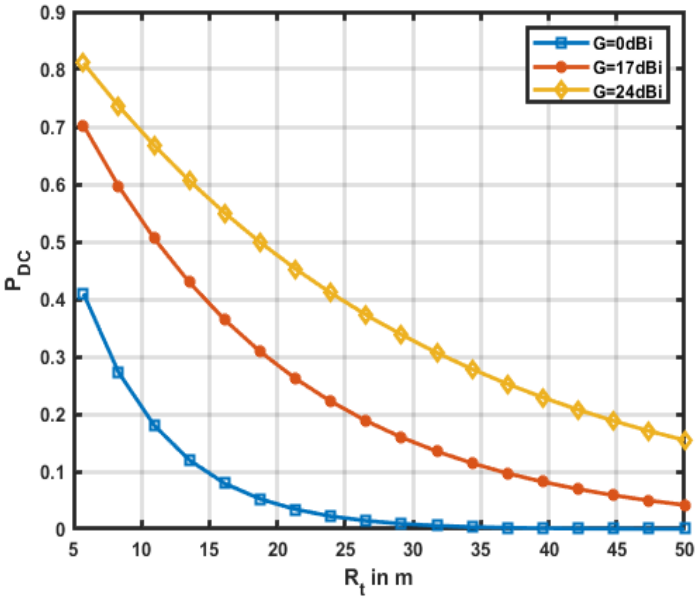

a. LOS

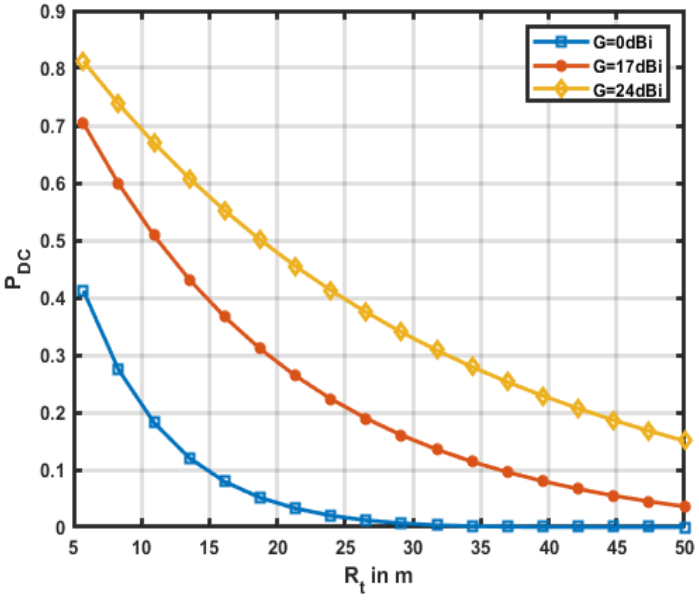

b. NLOS

FIGURE 4.5: Variation of P_{DC} with radar antenna gain. Remaining radar parameters and clutter parameters are kept fixed.

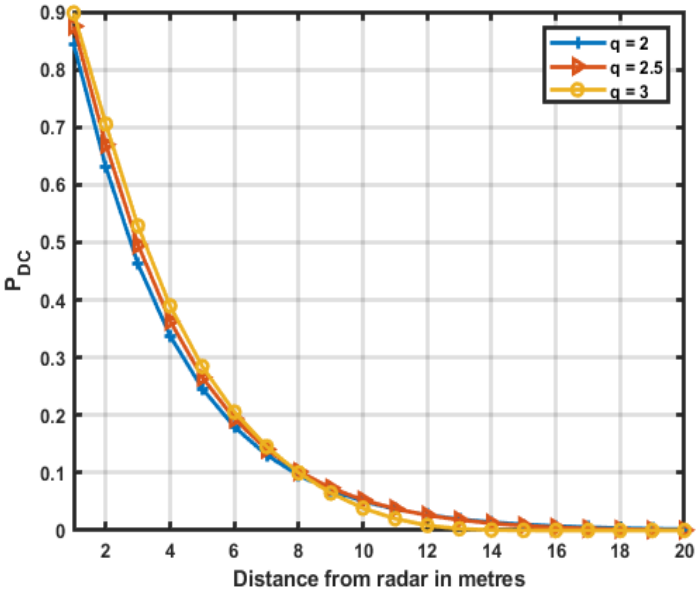

a. LOS

Also, the clutter backscatter reduces with the fall in the number of clutter scatterers within the main lobe of the radar antennas. Very similar results are obtained for the NLOS scenario as observed in Fig. 4.5b.

All the results presented so far have been generated with the assumption that the path loss coefficient is 2. Reflections from ground and ceiling may give rise to slightly higher path loss coefficients. The effect of q on P_{DC} is presented in Fig.4.6.

The results show that the there is insignificant variation in the performance of the radar for different values of q for both LOS (Fig. 4.6a) and NLOS scenarios (Fig. 4.6b).

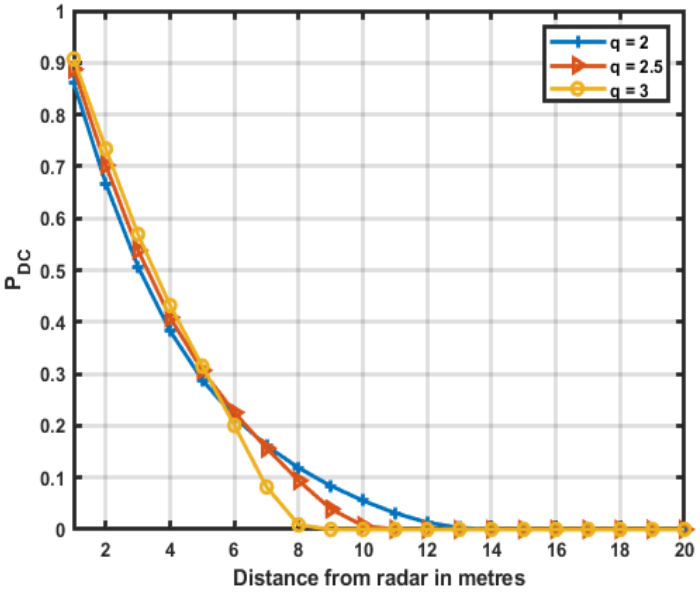

b. NLOS

FIGURE 4.6: Variation of P_{DC} with path loss coefficients. Remaining radar parameters and clutter parameters are kept fixed.

Chapter 5

Validation of Stochastic Geometry Results

The results obtained gave an insight on the parameters and the figure of merit P_{DC} variation. To validate the results we used Monte Carlo simulations and Finite Difference Time Domain (FDTD) methods.

5.0.1 Monte Carlo

We reproduced the results for Bandwidth variation in Stochastic Geometry and ran Monte Carlo simulation to validate. Results shown in Fig. 5.1 are produced for clutter density of 0.05 and at a distance of $10m$ from the Radar. We ran a series of Monte Carlo simulations consisting of 200000 trials to validate the stochastic geometry results. The figure shows excellent agreement between the Monte Carlo simulations and the results derived from stochastic geometry based formulations.

5.0.2 FDTD

Finite Difference Time Domain is computational modelling technique of electromagnetic waves interacting with occlusions. The occlusions in our study are clutter points distributed in a two dimensional plane. We have defined the number of clutter points, their size, the distribution and the electromagnetic properties. One such instance of clutter distribution is shown in Fig. 5.2. The clutter density is kept $\rho = 0.05$, $\sigma_{c_{avg}} = 0.2m^2$, and material conductivity is kept 3.9 x $10^{-3}\mho m{-}1$. The source in FDTD simulations is narrowband with 1000 MHz bandwidth. From the FDTD simulations we have calculated the path loss incurred and used it to calculate the signal strength, further P_{DC}. We

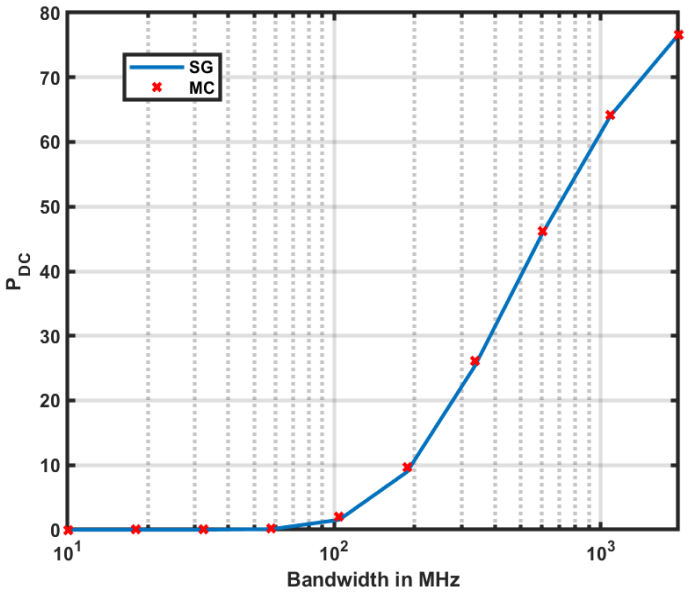

FIGURE 5.1: Validation of Stochastic Geometry results through Monte Carlo Simulations.

have compared the results with the Monte Carlo simulations, which follow it perfectly as shown in Fig 5.3.

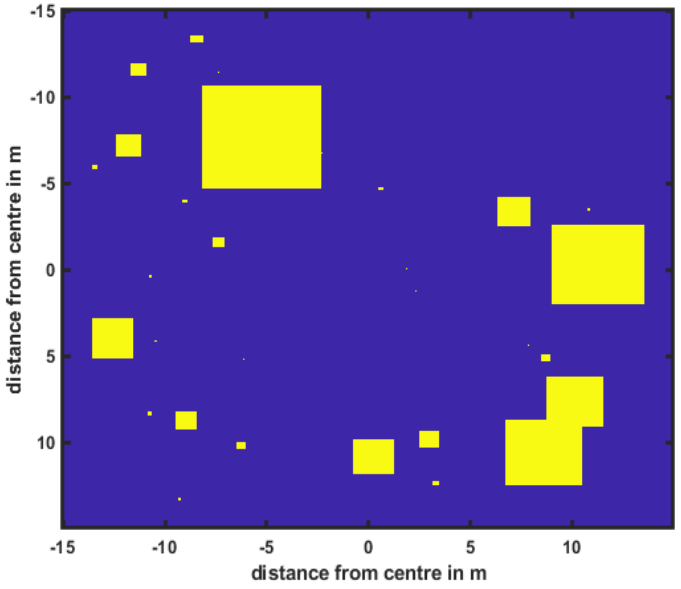

FIGURE 5.2: Clutter Instance in FDTD for $\rho = 0.05$

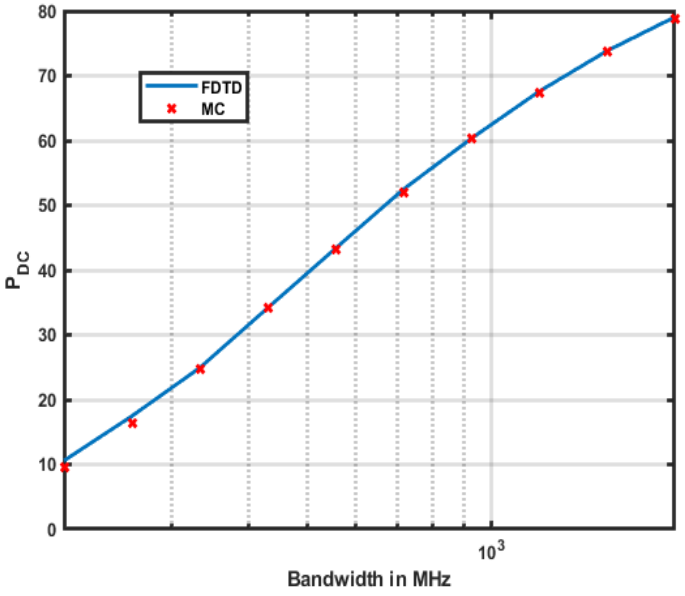

FIGURE 5.3: Validation of P_{DC} variation against Bandwidth in FDTD simulation with the results of Monte Carlo.

Chapter 6

Conclusion

We have provided a new figure of merit called the radar detection coverage probability to gauge the performance of a radar in a cluttered environment where the constituents of the clutter are discrete scatterers of cross-sections comparable to the target. We have provided an analytical framework for estimating $P_{DC}(r)$ using stochastic geometry formulations while incorporating the statistical characteristics of the radar, channel and target parameters. We provided the results for two cases - when the target is within the line of sight of the radar and when the target is blocked or shadowed by the clutter. The metric offers some key insights into the choice of radar parameters required for optimizing the performance of the system. (1) Unlike noise limited scenarios, in clutter limited scenarios, increase in transmitted power does not result in corresponding improvement of radar detection performance. (2) Radar bandwidth reduces the clutter returns by reducing the range resolution size. However, the noise increases. Our formulations show the optimum bandwidth for obtaining peak performance. The stochastic geometry framework, thereby, provides a useful tool for estimating such parameters for optimum detection performance. We have provided a new figure of merit called the radar detection coverage probability to gauge the performance of a radar in a cluttered environment where the constituents of the clutter are discrete scatterers of cross-sections comparable to the target. We have provided an analytical framework for estimating $P_{DC}(r)$ using stochastic geometry formulations while incorporating the statistical characteristics of the radar, channel and target parameters. We provided the results for two cases - when the target is within the line of sight of the radar and when the target is blocked or shadowed by the clutter. The metric offers some key insights into the choice of radar parameters required for optimizing the performance of the system. (1) Unlike noise limited scenarios, in clutter limited scenarios, increase in transmitted power does not result in corresponding improvement of radar detection performance. (2) Radar bandwidth reduces the clutter returns by reducing the range resolution size. However,

the noise increases. Our formulations show the optimum bandwidth for obtaining peak performance. We have verified our results using Monte Carlo simulations and FDTD solver. The stochastic geometry framework, thereby, proves as a useful tool for estimating such parameters for optimum performance.

This work considered specific models for clutter and target radar cross sections. In further work different other models can be explored and a more generalised expression for detection coverage probability can be shown. Stochastic geometry results can also be validated through empirical methods and performance of suggested metric in actual radar deployments can be figured out.

Bibliography

[1] Merrill Ivan Skolnik. *Radar handbook, 3rd edition.* McGraw-Hill Education, 2008.

[2] Jenho Tsao and Bernard D Steinberg. Reduction of sidelobe and speckle artifacts in microwave imaging: The clean technique. *IEEE Transactions on Antennas and Propagation*, 36(4):543–556, 1988.

[3] Jian Li and Petre Stoica. Efficient mixed-spectrum estimation with applications to target feature extraction. *IEEE transactions on signal processing*, 44(2):281–295, 1996.

[4] Pawan Setlur, Tadahiro Negishi, Natasha Devroye, and Danilo Erricolo. Multipath exploitation in non-los urban synthetic aperture radar. *IEEE Journal of Selected Topics in Signal Processing*, 8(1):137–152, 2013.

[5] Fawwaz Ulaby, M Craig Dobson, and José Luis Álvarez-Pérez. *Handbook of radar scattering statistics for terrain.* Artech House, 2019.

[6] Martin Haenggi, Jeffrey G Andrews, François Baccelli, Olivier Dousse, and Massimo Franceschetti. Stochastic geometry and random graphs for the analysis and design of wireless networks. *IEEE Journal on Selected Areas in Communications*, 27(7): 1029–1046, 2009.

[7] Jeffrey G Andrews, François Baccelli, and Radha Krishna Ganti. A tractable approach to coverage and rate in cellular networks. *IEEE Transactions on communications*, 59(11):3122–3134, 2011.

[8] Tianyang Bai and Robert W Heath. Coverage and rate analysis for millimeter-wave cellular networks. *IEEE Transactions on Wireless Communications*, 14(2): 1100–1114, 2014.

[9] Gourab Ghatak, Antonio De Domenico, and Marceau Coupechoux. Coverage analysis and load balancing in hetnets with millimeter wave multi-rat small cells. *IEEE Transactions on Wireless Communications*, 17(5):3154–3169, 2018.

[10] Zhen Tong, Hongsheng Lu, Martin Haenggi, and Christian Poellabauer. A stochastic geometry approach to the modeling of dsrc for vehicular safety communication. *IEEE Transactions on Intelligent Transportation Systems*, 17(5):1448–1458, 2016.

[11] A. Al-Hourani, R. J. Evans, S. Kandeepan, B. Moran, and H. Eltom. Stochastic geometry methods for modeling automotive radar interference. *IEEE Transactions on Intelligent Transportation Systems*, 19(2):333–344, Feb 2018. doi: 10.1109/TITS.2016.2632309.

[12] Andrea Munari, Ljiljana Simić, and Marina Petrova. Stochastic geometry interference analysis of radar network performance. *IEEE Communications Letters*, 22 (11):2362–2365, 2018.

[13] Sung Nok Chiu, Dietrich Stoyan, Wilfrid S Kendall, and Joseph Mecke. *Stochastic geometry and its applications*. John Wiley & Sons, 2013.

[14] X Chen, Ratnasingham Tharmarasa, Michel Pelletier, and Thia Kirubarajan. Integrated clutter estimation and target tracking using poisson point processes. *IEEE Transactions on Aerospace and Electronic Systems*, 48(2):1210–1235, 2012.

[15] Merrill Ivan Skolnik. Introduction to radar systems. *New York, McGraw Hill Book Co., 1980. 590 p.*, 1980.

[16] Oliver Rabaste, ELise Colin-Koeniguer, Dominique Poullin, Anil Cheraly, Jean-Francois Petex, and Huy-Khang Phan. Around-the-corner radar: Detection of a human being in non-line of sight. *IET Radar, Sonar Navigation*, 9(6):660–668, 2015.